Eng. & Technology, Vol.24, No. 7, 2005

A Three-Dimensional Study of Laminar and Turbulent Wall Jets

Talib K. Murtadha*

Received on:7/1/2003
Accepted on: 18/7/2005

Abstract

A numerical study of three-dimensional laminar and turbulent wall jet issuing from a rectangular orifice is presented. The numerical simulation was based on k-ε model. The Navier-Stokes, energy, and turbulence quantities are solved using the finite difference primitive variable method with staggered grid technique. The flow field characteristics are studied in laminar flow for Reynolds numbers up to 3000 and in turbulent flow for Reynolds numbers up to 56000. The results show that the spreading rate of the jet is higher at low Reynolds numbers and the decay of axial velocity is less at high Reynolds numbers. The numerical results obtained are compared with published experimental results and found to be in reasonable agreement.

دراسة عددية لنفاث الجدار (الطباقي والاضرابي) الثلاثي الأبعاد

الخلاصة

تضمن هذا البحث دراسة عددية لنفاث الجدار (الخارج من فتحة مستطيلة الشكل) الثلاثي الأبعاد في الجريان الطباقي والاضطرابي. تأثير الاضراب على الجريان تمت دراسته باستخدام نموذج (k-ε) . تم حل المعادلات المتعلقة بجريان المائع (Navier-stokes equations) ، ومعادلة الطاقة (Energy equation) باستخدام طريقة الفروق المحددة وبطريقة المتغيرات الأولية المعتمدة على تقنية الشبكة الزاحفة. خصائص حقل الجريان تمت دراستها لأرقام رينولدز وصلت إلى 3000 في الجريان الطباقي بينما أرقام رينولدز المدروسة في الجريان الأضطرابي وصلت إلى 56000 . بينت النتائج أن معدل الانتشار للنفاث يكون أعلى في أرقام رينولدز الواطئة وأن اضمحلال السرعة المحورية أقل عند الأرقام العالية . كذلك بينت النتائج أن درجات الحرارة تكون عالية بالقرب من الجدار. قورنت النتائج العددية مع النتائج التجريبية المنشورة وكان التوافق مرضياً .

Nomenclature

b	: Orifice breadth	m
c_μ, $c_{1\varepsilon}$, $c_{2\varepsilon}$	: Constants in turbulence model	-
D_h	: Hydraulic diameter	m
e	: Aspect ratio of jet=b/h	-
h	: Width of orifice	m
k	: Turbulent kinetic energy = $\frac{1}{2}\left(\overline{u'^2} + \overline{v'^2} + \overline{w'^2}\right)$	m^2/s^2
P	: Mean static pressure, P	N/m^2
Re	: Reynolds number = $\frac{U_o.D_h}{\nu}$	-
U	: Mean velocity in the x-direction	m/s
V	: Mean velocity in the y-direction	m/s

* Dept. of Mechanical Eng., UOT.

https://doi.org/10.30684/etj.24.7A.3
2412-0758/University of Technology-Iraq, Baghdad, Iraq

W	: Mean velocity in the z-direction	m/s
x,y,z	: Cartesian Coordinates	m
X,Y,Z	: Dimensionless Cartesian Coordinate	-
y^+	: Dimensionless Coordinates $y^+ = (y_p / \nu)\sqrt{\tau_w / \rho}$	-
θ	: Dimensionless temperature, $\frac{T - T_w}{T_a - T_w}$	-
ε	: Dissipation rate of turbulent kinetic energy	m^2/sec^2
ρ	: Density of air	kg/m^3
σ_k, σ_ε	: Turbulent prandil numbers for k, ε	-
μ	: Dynamic viscosity	$N.s/m^2$
ν	: Kinematic viscosity	m^2/s
ν_t	: Eddy or turbulent viscosity	-
ν_e	: Effective kinematics viscosity	-
Γ	: Diffusion coefficient, $\Gamma=\mu/\sigma$	$N.s/m^2$
Γ_e	: Effective diffusion coefficient, $\Gamma_e=\mu_e/\sigma_e$	$N.s/m^2$
k	: Von Karman's constant	-
τ_w	: Wall shear stress	N/m^2
ϕ	: General dependent variable	
S_ϕ	: Source term	

Introduction

A wall jet has a wide range of applications such as gas turbines film cooling, aircraft blow down flap and in heating and air conditioning practice. The wall jet has been studied both experimentally and theoretically (1-11). In these studies the plane wall jet characteristics were studied in turbulent flow for different configurations. The present work is directed towards examining the flow field of three dimensional heated wall jet flow on a flat surface in laminar and turbulent flow.

The algorithm SIMPLE (12) was used in this work to study the problem with the Navier-Stokes equations written in terms of primitive variable method. The problem to be considered in this study is depicted Fig.(1). The geometry is specified by the orifice width h, and the aspect ratio e. The governing equations to be considered are the continuity, momentum, energy and turbulence quantities. The numerical prediction was based on staggered grid techniques where the vector variables are staggered midway between the grid intersections.

Theory

The flow field is assumed to be three-dimensional with constant properties, and the buoyancy effect is neglected. The governing equations can be expressed in the following conservative form as:

i) Laminar flow

$$\frac{\partial U}{\partial X} + \frac{\partial V}{\partial Y} + \frac{\partial W}{\partial Z} = 0 \qquad (1)$$

$$U\frac{\partial U}{\partial X} + V\frac{\partial V}{\partial Y} + W\frac{\partial W}{\partial Z} = -\frac{\partial P}{\partial X} + \frac{1}{Re}\left(\frac{\partial^2 U}{\partial X^2} + \frac{\partial^2 U}{\partial Y^2} + \frac{\partial^2 U}{\partial Z^2}\right) \qquad (2)$$

$$U\frac{\partial V}{\partial X}+V\frac{\partial V}{\partial Y}+W\frac{\partial V}{\partial Z}= -\frac{\partial P}{\partial Y}+\frac{1}{Re}\left(\frac{\partial^2 V}{\partial X^2}+\frac{\partial^2 V}{\partial Y^2}+\frac{\partial^2 V}{\partial Z^2}\right) \quad (3)$$

$$U\frac{\partial W}{\partial X}+V\frac{\partial W}{\partial Y}+W\frac{\partial W}{\partial Z}= -\frac{\partial P}{\partial Z}+\frac{1}{Re}\left(\frac{\partial^2 W}{\partial X^2}+\frac{\partial^2 W}{\partial Y^2}+\frac{\partial^2 W}{\partial Z^2}\right) \quad (4)$$

$$U\frac{\partial \theta}{\partial X}+V\frac{\partial \theta}{\partial Y}+W\frac{\partial \theta}{\partial Z}= \frac{1}{Pe}\left(\frac{\partial^2 \theta}{\partial X^2}+\frac{\partial^2 \theta}{\partial Y^2}+\frac{\partial^2 \theta}{\partial Z^2}\right) \quad (5)$$

ii) Turbulent flow

In turbulent flow, the mean flow equations can be expressed for steady state conditions as follows:

$$U\frac{\partial U}{\partial X}+V\frac{\partial U}{\partial y}+W\frac{\partial U}{\partial z}= -\frac{1}{\rho}\frac{\partial P}{\partial X}+\frac{\partial}{\partial X}\left(v_e\frac{\partial U}{\partial x}\right)+\frac{\partial}{\partial Y}\left(v_e\frac{\partial U}{\partial y}\right)+\frac{\partial}{\partial z}\left(v_e\frac{\partial U}{\partial z}\right)+\frac{\partial}{\partial X}\left(v_e\frac{\partial U}{\partial x}\right)+\frac{\partial}{\partial y}\left(v_e\frac{\partial V}{\partial x}\right)+\frac{\partial}{\partial Z}\left(v_e\frac{\partial W}{\partial x}\right) \quad (6)$$

$$U\frac{\partial V}{\partial x}+V\frac{\partial V}{\partial y}+W\frac{\partial V}{\partial z}= -\frac{1}{\rho}\frac{\partial P}{\partial y}+\frac{\partial}{\partial x}\left(v_e\frac{\partial V}{\partial x}\right)+\frac{\partial}{\partial y}\left(v_e\frac{\partial V}{\partial y}\right)+\frac{\partial}{\partial z}\left(v_e\frac{\partial V}{\partial z}\right)+\frac{\partial}{\partial x}\left(v_e\frac{\partial U}{\partial y}\right)+\frac{\partial}{\partial y}\left(v_e\frac{\partial V}{\partial y}\right)+\frac{\partial}{\partial z}\left(v_e\frac{\partial W}{\partial y}\right) \quad (7)$$

$$U\frac{\partial W}{\partial x}+V\frac{\partial W}{\partial y}+W\frac{\partial W}{\partial z}= -\frac{1}{\rho}\frac{\partial P}{\partial z}+\frac{\partial}{\partial x}\left(v_e\frac{\partial W}{\partial x}\right)+\frac{\partial}{\partial y}\left(v_e\frac{\partial W}{\partial y}\right)+\frac{\partial}{\partial z}\left(v_e\frac{\partial W}{\partial z}\right)+\frac{\partial}{\partial x}\left(v_e\frac{\partial U}{\partial z}\right)+\frac{\partial}{\partial y}\left(v_e\frac{\partial V}{\partial z}\right)+\frac{\partial}{\partial z}\left(v_e\frac{\partial W}{\partial z}\right) \quad (8)$$

To solve the governing equations (6-8) a mathematical expression for effective kinematic viscosity v_e and effective diffusion coefficient Γ_e will be required in the consideration of turbulence.

The Standard k-ε Model

The k-ε Model characterizes the local state of turbulence by two parameters: the turbulent kinetic energy, k and the rate of its dissipation, ε. The kinematic viscosity is related to these parameters by Kolmogrov-Prandtl expression [15]:

$$v_t = c_\mu \frac{K^2}{\varepsilon} \quad (9)$$

where c_μ is an empirical constant. The distribution of k and ε over the flow field is calculated from the following semi-empirical transport equations for k and ε [16].

$$\frac{\partial Uk}{\partial x}+\frac{\partial Vk}{\partial y}+\frac{\partial Wk}{\partial z}=\frac{\partial}{\partial x}\left(\frac{v_t}{\sigma_k}\frac{\partial k}{\partial x}\right)+\frac{\partial}{\partial y}\left(\frac{v_t}{\sigma_k}\frac{\partial k}{\partial y}\right)+\frac{\partial}{\partial z}\left(\frac{v_t}{\sigma_k}\frac{\partial k}{\partial z}\right)$$
$$+v_t\left[\begin{array}{l}2\left(\frac{\partial U}{\partial x}\right)^2+2\left(\frac{\partial V}{\partial y}\right)^2+2\left(\frac{\partial W}{\partial z}\right)^2+\left(\frac{\partial U}{\partial y}+\frac{\partial V}{\partial x}\right)^2+\\ \left(\frac{\partial U}{\partial z}+\frac{\partial W}{\partial x}\right)^2+\left(\frac{\partial V}{\partial z}+\frac{\partial W}{\partial y}\right)^2\end{array}\right]-\varepsilon \qquad (10)$$

$$\frac{\partial U\varepsilon}{\partial x}+\frac{\partial V\varepsilon}{\partial y}+\frac{\partial W\varepsilon}{\partial z}=\frac{\partial}{\partial x}\left(\frac{v_t}{\sigma_\varepsilon}\frac{\partial \varepsilon}{\partial x}\right)+\frac{\partial}{\partial y}\left(\frac{v_t}{\sigma_\varepsilon}\frac{\partial \varepsilon}{\partial y}\right)+\frac{\partial}{\partial Z}\left(\frac{v_t}{\sigma_\varepsilon}\frac{\partial \varepsilon}{\partial z}\right)$$
$$+C_{1\varepsilon}\frac{\varepsilon}{k}v_t\left[\begin{array}{l}2\left(\frac{\partial U}{\partial x}\right)^2+2\left(\frac{\partial V}{\partial y}\right)^2+2\left(\frac{\partial W}{\partial z}\right)^2+\left(\frac{\partial U}{\partial y}+\frac{\partial V}{\partial x}\right)^2+\\ \left(\frac{\partial U}{\partial z}+\frac{\partial W}{\partial x}\right)^2+\left(\frac{\partial V}{\partial z}+\frac{\partial W}{\partial y}\right)^2\end{array}\right]-C_{2\varepsilon}\frac{\varepsilon^2}{k} \qquad (11)$$

where

$$v_t\left[\begin{array}{l}2\left(\frac{\partial U}{\partial x}\right)^2+2\left(\frac{\partial V}{\partial y}\right)^2+2\left(\frac{\partial W}{\partial z}\right)^2+\left(\frac{\partial U}{\partial y}+\frac{\partial V}{\partial x}\right)^2+\\ \left(\frac{\partial U}{\partial z}+\frac{\partial W}{\partial x}\right)^2+\left(\frac{\partial V}{\partial z}+\frac{\partial W}{\partial y}\right)^2\end{array}\right]$$

is the generation term G, ε is the dissipation term.

The empirical constants appearing in the above model are shown in the following table.

Table (1) Empirical constants in the k-ε [16]

C_μ	$C_{1\varepsilon}$	$C_{2\varepsilon}$	σ_k	σ_ε
0.09	1.44	1.92	1.00	1.30

Boundary Conditions

The boundary conditions for the problem under consideration can be described for laminar and turbulent flow as follows:

(i) Laminar Flow

At the free edges (entrainment region):

$$\frac{\partial U}{\partial y}=0,\frac{\partial V}{\partial y}=0,\frac{\partial W}{\partial y}=0,\frac{\partial T}{\partial y}=0,P=0$$

The velocity of the jet at the free edge may reach the static surrounding velocity (u=0) or $\frac{\partial U}{\partial y}=0$. The static pressure within the jet is the same as the static pressure of the surrounding ($\frac{\partial P}{\partial x}$ is negligible) if the surrounding at constant velocity, i.e at rest.

At the wall:

* Dept. of Mechanical Eng., UOT.

$$U = V = W = 0, \frac{\partial P}{\partial y} = 0, \frac{\partial \theta}{\partial y} = 0$$

To ensure smooth transition at the last stream wise station of the combined jet, the following boundary conditions are used:

$$\frac{\partial^2 U}{\partial x^2} = \frac{\partial^2 V}{\partial x^2} = \frac{\partial^2 W}{\partial x^2} = 0$$

(ii) Turbulent flow

$$\frac{\partial U}{\partial y} = 0, \frac{\partial V}{\partial y} = 0, \frac{\partial W}{\partial y} = 0,$$
$$\frac{\partial T}{\partial y} = 0, K = 0, \varepsilon = 0$$

Wall boundary

The implementation of the wall boundary conditions in turbulent flow starts with evaluation of:

$$y^+ = \frac{y_p}{\nu}\sqrt{\frac{\tau_w}{p}} \qquad (12)$$

where y_p is the distance of near wall node p to the solid surface. A near wall flow is assumed to be laminar if $y^+ \leq 11.6$ and turbulent if $y^+ > 11.63$ [14].

Constant shear stress (τ_w) will be assumed through the wall region:

$\tau_w = \mu \frac{U_p}{y_p}$ where U_p is the velocity at the grid node near the surface.

The wall force is represented in the discretized U-momentum equation as follows:

$$F_s = -\tau_w A_{cell} \qquad (13)$$

Where A_{cell} is the wall area of the control volume.

U-velocity parallel to the wall:

The wall force F_s is introduced in to the discretized U-equation as source term, so

$$S_p = -\frac{\mu}{y_p} A_{cell} \quad for \quad y^+ \leq 11.63 \qquad (14)$$

$$S_p = -\frac{pC_\mu^{1/4} K_p^{1/2} k}{Ln(Ey^+)} \quad for \quad y^+ > 11.63 \qquad (15)$$

Where:-
Sp = Source term for turbulent flow,
K = Von Karman's constant (0.4187),
E = logarithmic wall constant (9.79),
kp = turbulent kinetic energy for node p,
C_μ = empirical constant (0.09)[14].

Turbulence quantities
K-equation:

The source terms for the turbulent flow in the discretized k-equation are represented as:

$$S_p = -\rho C_\mu^{3/4} K_p^{1/2} Ln\left(\frac{Ey^+}{ky_p}\right)\Delta V \qquad (16)$$
$$and \; S_u = \frac{-\tau_w U_p}{y_p}\Delta V$$

where ΔV is the wall volume of control volume.

ε-equation:

The discretized ε-equation is fixed to the value:

$$\varepsilon_p = \frac{C_\mu^{3/4} K_p^{3/2}}{(ky_p)} \qquad (17)$$

in the discretized ε-equation the near wall node is fixed to the given value in equation (17) by means of setting the source terms S_p and S_u as follows [14]:-

$$S_p = -10^{30} \quad and$$

$$S_u = \frac{C_\mu^{3/4} K_p^{3/2}}{(ky_p)} x10^{30} \qquad (18)$$

Temperature equation

The wall heat flux is introduced by the means of the following [14] source terms

$$S_p = \frac{-\rho C_\mu^{1/4} K_p^{1/2} C_p}{T^+} A_{cell}$$

$$and \qquad (19)$$

$$S_u = \frac{\rho C_\mu^{1/4} k_p^{1/2} C_p T_w}{T^+} A_{cell}$$

where:

$$T^+ = \sigma_t \left[\frac{1}{k} ln(Ey^+) + P\left(\frac{\sigma_L}{\sigma_t}\right) \right] \qquad (20)$$

σ_t, σ_L is the turbulent and laminar Prandtl number.

$P\left(\frac{\sigma_L}{\sigma_t}\right)$ is called the Pee-function.

Here, for the considered adiabatic walls $S_p = S_u = 0$.

Therefore, at the walls the following boundaries are considered:

$U=V=W=0$

$$\frac{\partial K}{\partial y} = 0, \frac{\partial \varepsilon}{\partial y} = 0, \frac{\partial T}{\partial y} = 0$$

Numerical Solution

Numerical procedure called SIMPLE (semi-implicit method for pressure-linked equations) is used to solve the basic conservative equations. This procedure of Patankar and Spalding is found in ref.[12]. The finite difference mesh consists of many control volumes using a staggered grid system. All scalar variables (such as pressure and temperature) are defined at ordinary nodal points, the velocity components are defined on staggered grids centered around the cell faces, see Fig.(2). Let ϕ be any dependent variable for which the conservation equation is as follows:

$$\frac{\partial U\Phi}{\partial x} + \frac{\partial V\Phi}{\partial y} + \frac{\partial W\Phi}{\partial z} =$$

$$\frac{\partial}{\partial x}\left(\Gamma \frac{\partial \Phi}{\partial x}\right) + \frac{\partial}{\partial y}\left(\Gamma \frac{\partial \Phi}{\partial y}\right) + \qquad (21)$$

$$\frac{\partial}{\partial z}\left(\Gamma \frac{\partial \Phi}{\partial z}\right) + S_\Phi$$

where S_Φ is the source term which has different expressions for different flow equations. After applying central difference for the diffusion terms and upwind difference for convective terms the above equations are discritized (reduced to algebraic equations) and solved numerically. The discretization equation connects the values of Φ for a group of grid points, usually the grid points of the control volume as follows:

$$A_J \Phi_J = A_E \Phi_E + A_W \Phi_W + A_N \Phi_N +$$

$$A_S \Phi_S + A_B \Phi_B + A_T \Phi_T + S_\Phi$$

where each coefficient in the above equation includes convective and diffusion term.

The pressure is corrected to satisfy continuity at the end of each iteration. To derive the pressure correction equation we define the following:

$P=P^*+P'$; $U=U^*+U'$;
$V=V^*+V'$; $W=W^*+W'$

where, the starred values (U*, V*) represent the flow solution given by the pressure (P*). By applying the above in the discretized momentum and continuity equations and simplifying, a linear system can be obtained for P' (Pressure correction) in solving the steady momentum equations in this step. Under relaxation factors were used to the component of the velocity, pressure, heat, and turbulent equations to prevent instability and divergence due to nonlinearity in the Navier-stokes equations.

Results and Discussion

Results are obtained numerically for incompressible flow under the conditions illustrated in the forgoing sections. The flow field and thermal characteristics for different Reynolds number and different aspect ratios are discussed separately.

Flow Field

Effect of Reynolds number on the flow field distribution is seen in figs.(3-4) for laminar and turbulent flow. It can be seen that boundary layer growth on surface meets the shear layer expansion on the free boundary because the wall jet extract some of the static surrounding fluid that leads to form a mixing region between the boundary layer on surface and the static fluid, finally creasing spreading in the down stream direction. As fig.(3) shows, the spreading rate of the wall jet at low Reynolds numbers, because at the low Reynolds number the jet extract more static fluid leading to increase the interaction between the wall boundary layer growth and the free shear layer. Consequently it increases the spreading rate. The figure also shows that the decay of the axial velocity is less at high Reynolds number. In turbulent flow fig.(4), the decay of maximum axial velocity is less at high Reynolds number also the spreading rate of the wall jet in this flow is less from the laminar flow because of the high velocity.

Fig.(5) exhibits the effect of aspect of aspect ratio on the axial velocity distribution in the lateral direction (plane parallel to the solid surface). It can be seen that the aspect ratio has noticeable influence on the velocity distribution, where non-uniform distribution occurs with increasing of the aspect ratio and that may be attributed to the increase of turbulence, also the values of axial velocity is higher at larger aspect ratio.

Thermal Characteristics

The predicted isotherm contours for laminar flow are illustrated in fig.(6). The results show that the decay of axial temperature is less at high Reynolds number because the thermal boundary layer growth on solid surface is faster than that with the surrounding.

The effect of Reynolds number on temperature distribution in turbulent flow is seen in fig.(7). It can be seen that the thermal layer grow with down stream distance due to difference between the hot stream of the wall jet and that of the solid wall and surrounding. There is higher values of axial temperatures near the solid surface because of the friction induced between the flow and this surface which leads to increase of temperature. The spreading rate of thermal layer is decreased with increase of Reynolds number.

The computed results are compared with the published experimental results taken from [12] as shown in fig.(8). The comparison indicates a moderate agreement between results.

Fig.(9) exhibits the turbulent kinetic energy (which represents the intensity of turbulence fluctuations) for different aspect ratio in the lateral direction.

The peaks of the jet region increased in the lateral direction for the low aspect ratio. This significant difference between the studied aspect ratios may be attributed to differences in production, transport and dissipation of turbulent kinetic energy of the wall jet.

Conclusions

1. The spreading rate of the wall jet in turbulent flow is less than of that in laminar flow.
2. There is higher values of axial temperatures near the solid surface.
3. The spreading rate of thermal layer decreases with increasing Reynolds number.
4. The aspect ratio has noticeable effects on flow field and turbulence characteristics.

References

1. Myers, G.E., Schauer, J.J., Eustis R.H., "Heat Transfer to plane turbulent wall jets", ASME Journal of Heat Transfer. Aug.1963.
2. P.Y. Nizou, "Heat and Momentum Transfer in a Plane Turbulent Wall Jet", Transactions of ASME, Vol.103, Feb.1981.
3. Irwin, H.P., A.H., "Measurements in Self-Preserving Wall Jet in a Positive Pressure Gradient", Journal of Fluid Mechanics, Vol.61, 1973, pp.33-63.
4. J.B., Morton, *G.D.Catalano, and R.P.Humphris, "Some Two-Point Statistical Properties of a Three-Dimensional Wall Jet", AIAA Journal, Vol.16, No.7, July 1978.
5. G.P.,Hammaond, "Complete Velocity Profile And Optimum Skin Friction Formulas For The Plane Wall-Jet", Journal of Fluid Engineerings, Vol.104/59, March 1982.
6. L.F. Rossi, "Vortex Computations of Wall Jet Flows", 1st Annual Forum on Vortex Methods For Eng. Applications, Feb.1995.
7. Abrahamsson H., Johansson B; Lofdahl, "A Turbulent Plane Two-Dimensional Wall Jet In A Quiescent Surrounding", European Journal of Mechanics B-Fluids B:533-556, 1994.
8. Eriksson J., Karlsson R., Persson J., "Some New Results For The Turbulent Wall Jet With Focus On The Near-Wall Region", Proc.8th Int. Conf. on Laser Anemometry-Advances and Applications, University of Rome, Lasaprenza, Rome, Italy, 1999.
9. Eriksson J., Karlsson R., Persson J., "An Experimental Study of A Two-Dimensional Plane Turbulent Wall Jet", Exp. Fluids 25:50-60, 1998.
10. George W.K., Abrannssom H., Eriksson J., Wosnik M., "A Similarity Theory For The Turbulent Wall Jet Without External Stream. Submitted To Journal of Fluid Mechanics, 2000.
11. J.G. Eriksson and R.I. Karlsson, "Near-Wall Turbulence Structure In The Plane Turbulent Wall Jet In Still Surroundings", Royal Institute of Technology, 2001.
12. Patankar, S.V., "Numerical Heat Transfer and Fluid Flow", Mcgraw-Hill, New York, 1980.

13. Rajaratnam, N., "Turbulent Jets", Elsevier, 1976.
14. Versteeg and W. Malasekera, "An Introduction To Computational Fluid Dynamics, Longman Group Ltd, 1995.
15. Jones, W.P. and Lunder, B.E., "The Prediction of Laminarization With A Two Equation Model of Turbulence", Journal of Heat And Mass Transfer, Vol.15, 1972, Pp.301-314.
16. Launder, B.T. and Spalding, D.B., "Lecturers In Mathematical Models of Turbulence", Department of Mechanical Engineering, Imperial College of Science And Technology, London, England.

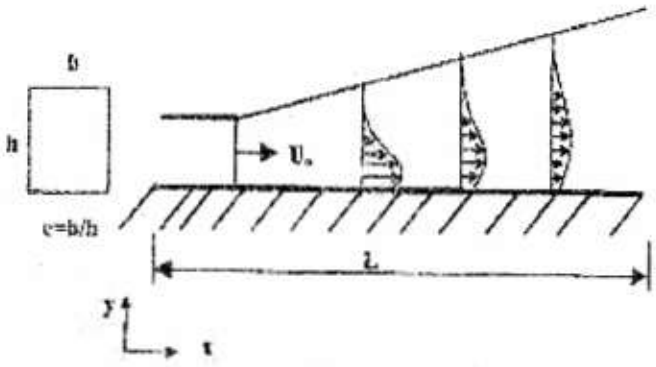

Fig.(1) Configuration of the problem.

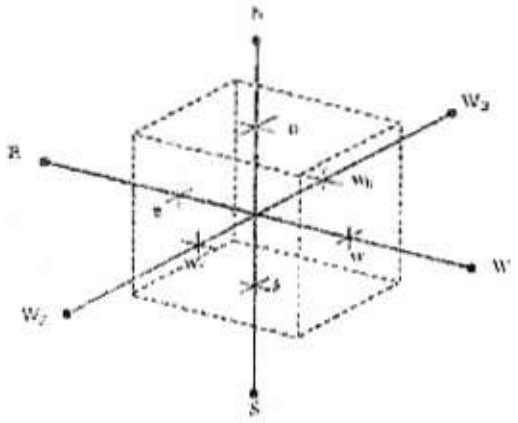

Fig.(2) Three-dimensional computational cell.

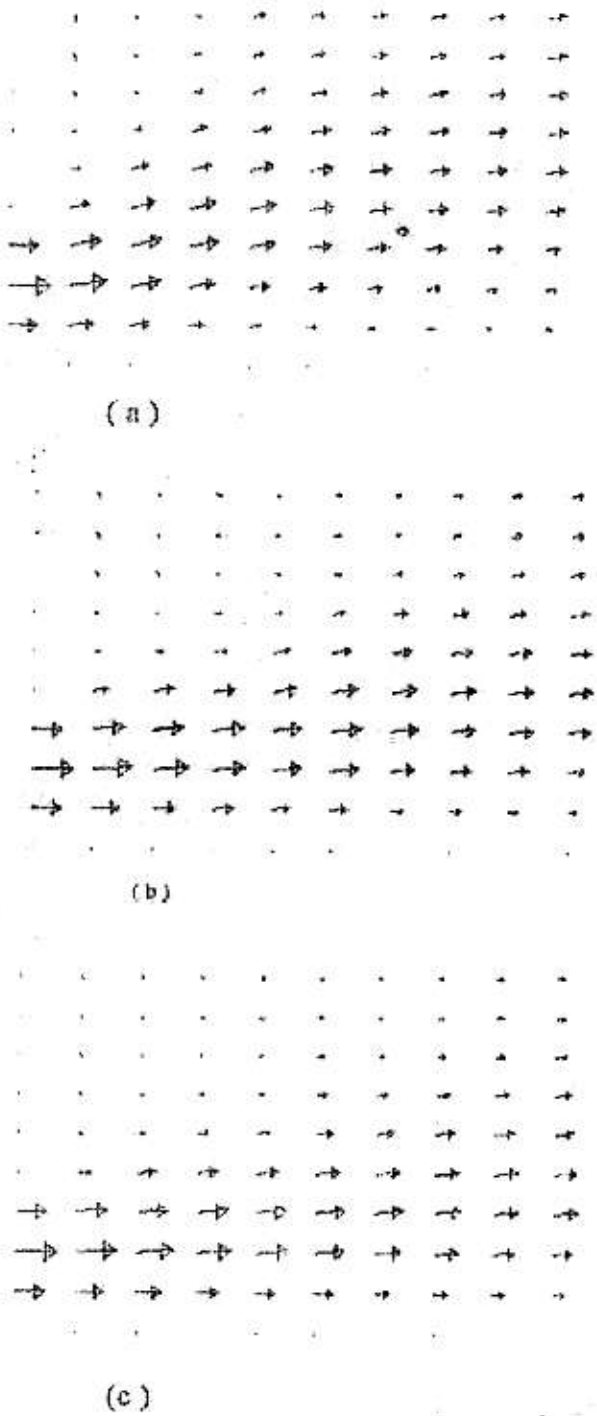

Fig.(3) Laminar flow field (U & V velocity vectors) for a. Re=1000, b. Re=2000, c. Re=3000 and e=3.

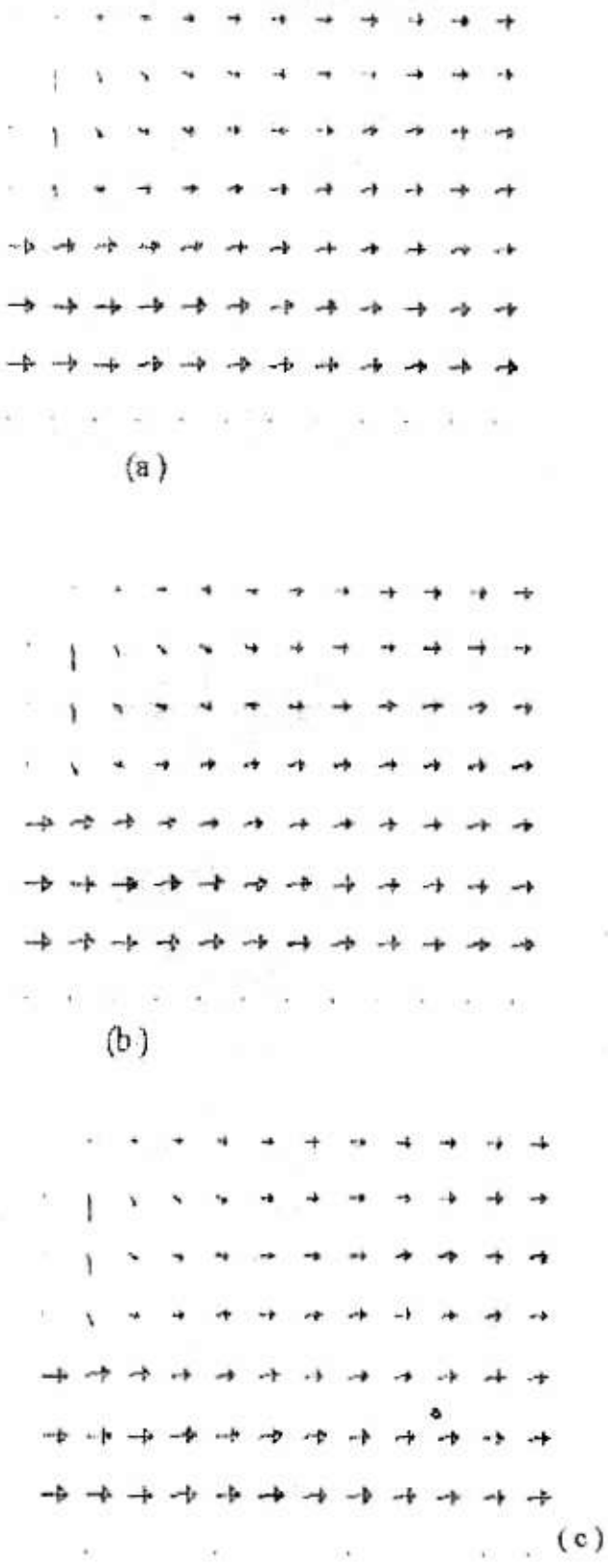

Fig.(4) 3-D Turbulent flow field (U & V velocity vectors) for a. $Re=2*10^4$, b. $Re=4*10^4$, c. $Re=5.7*10^4$ and e=3.

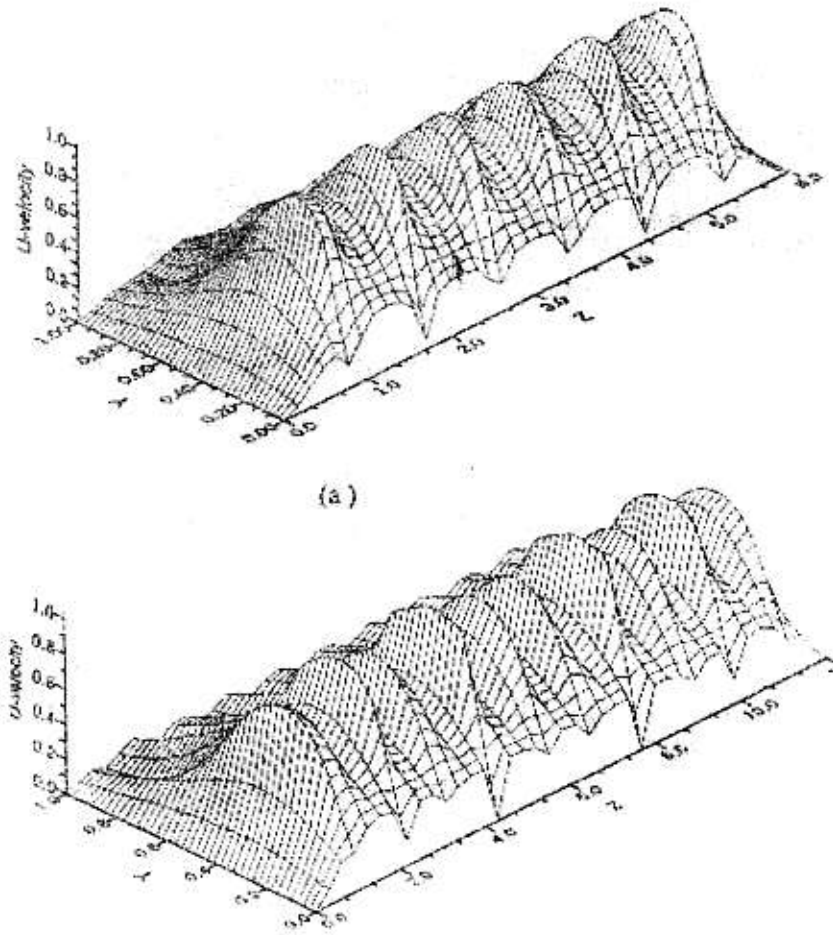

(a)

(b)

Fig.(5) Turbulent U-velocity distribution in lateral direction for different aspect ratio, a. e=3, b. e=6 with plane x=15.

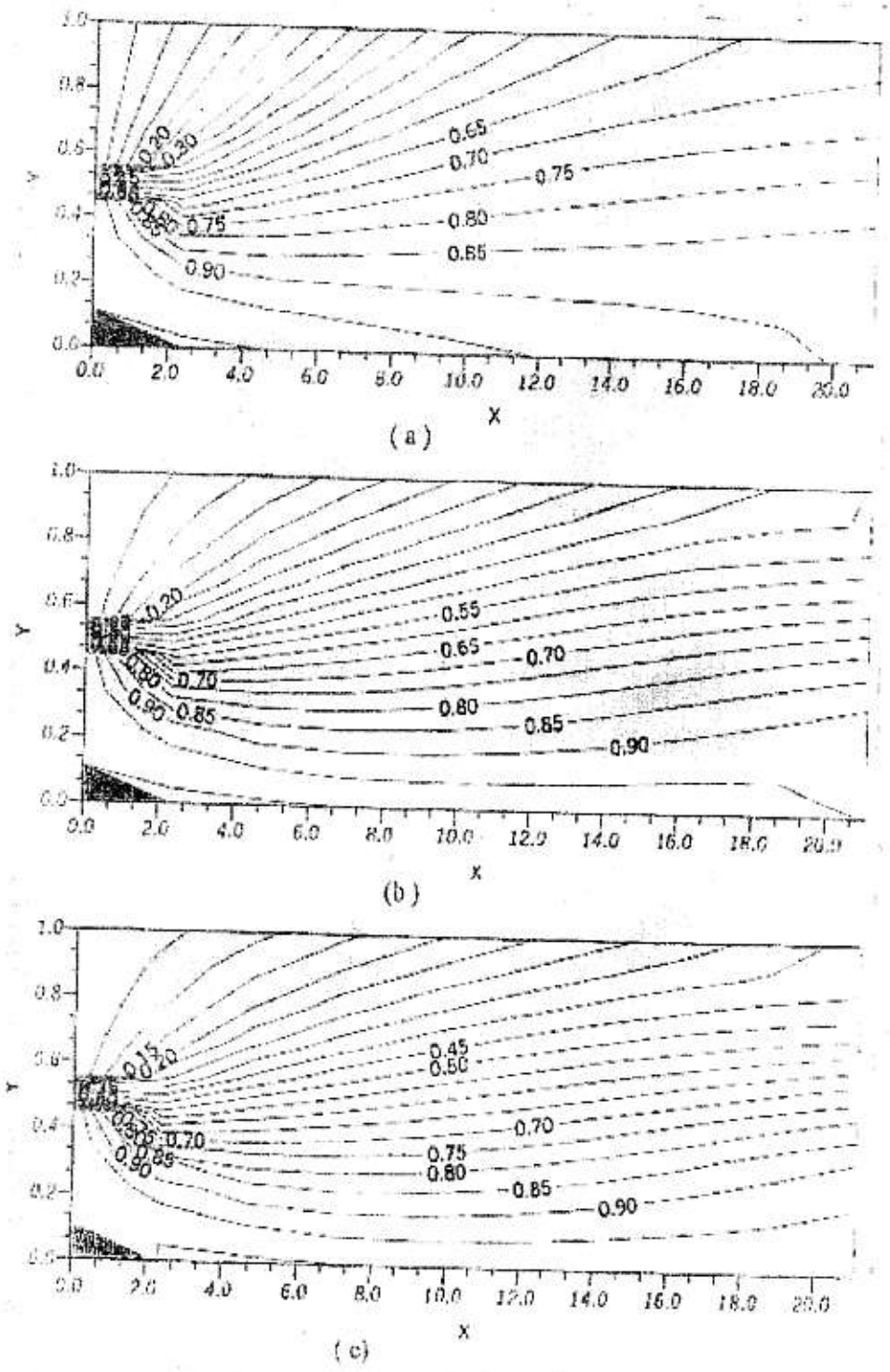

Fig.(6) Laminar isotherm contours for different Reynolds numbers a. Re=1000, b. Re=2000, c. Re=3000 and e=3.

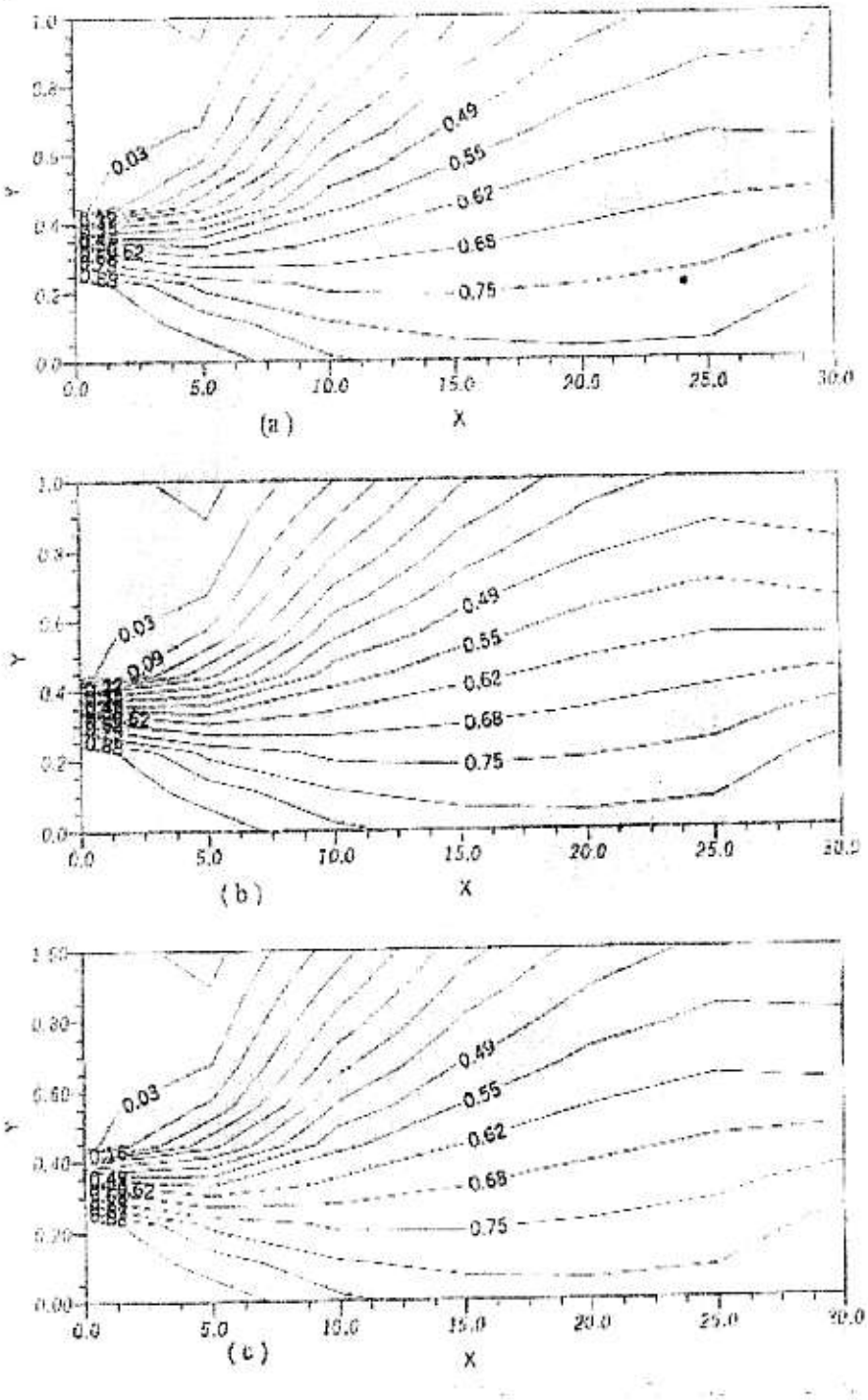

Fig.(7) Turbulent isotherm contours for different Reynolds numbers a.Re=20000, b. Re=40000, c. Re=57000 and e=3.

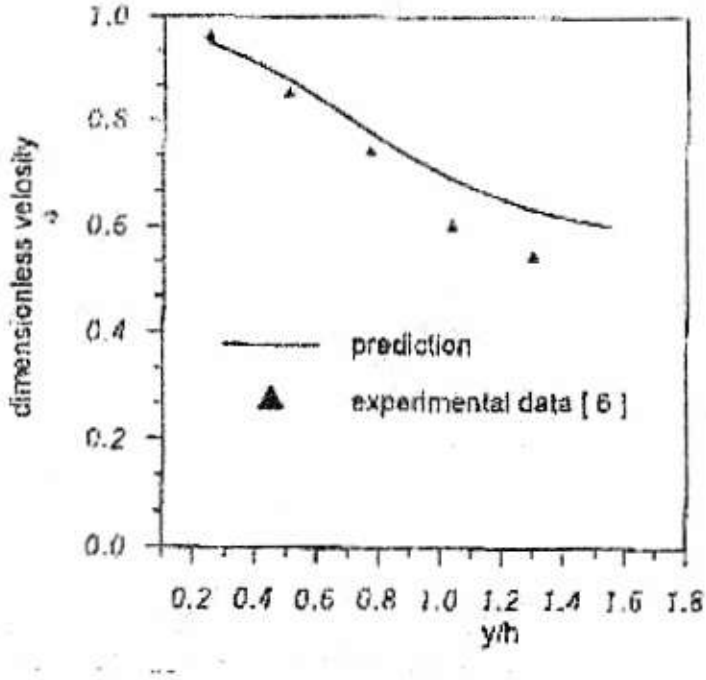

Fig.(8) Comparison of present numerical and published experimental results.

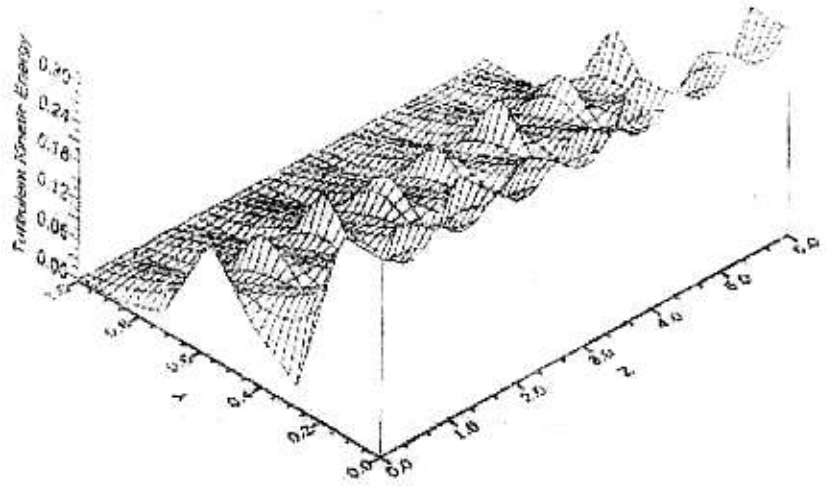

(a)

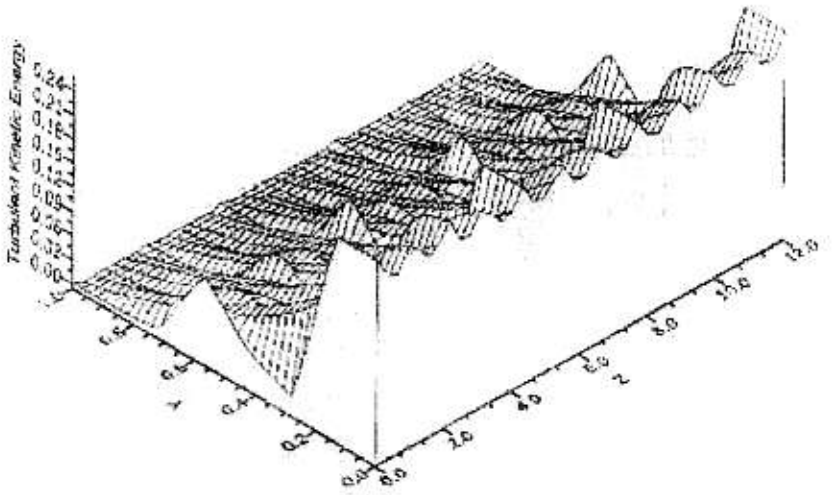

(b)

Fig.(9) Turbulent kinetic energy for different aspect ratio (a. e=3, b. e=6) Re=20000, with plane X=15 in lateral direction.